The Journal of Navigation (2023), **76**:2–3 181–199
doi:10.1017/S0373463323000085

CAMBRIDGE UNIVERSITY PRESS

RESEARCH ARTICLE

Collision risk quantification for pairs of recorded aircraft trajectories

Valtteri Kallinen,[1]* Steve Barry,[2] and Aaron McFadyen[1]

[1] School of Electrical Engineering and Robotics, Queensland University of Technology, Brisbane, Australia
[2] Airservices Australia, Canberra, Australia.
*Corresponding author: Steve Barry; Email: steven.ibarry@gmail.com

Received: 3 August 2021; **Accepted:** 12 March 2023; **First published online:** 26 April 2023

Keywords: risk; traffic management; aviation

Abstract

Complex domestic airspace requires collision risk models and monitoring tools suitable for arbitrary aircraft trajectories. This paper presents a new mathematically based collision risk approach that extends the International Civil Aviation Organisation (ICAO) models to full aircraft encounters based on real trajectory data. A new continuous time intervention model is presented, along with a position uncertainty propagation model that better reflects aircraft behaviour and allows generalisation to all trajectories to eliminate degenerate cases. The proposed risk model is computationally efficient compared to the models it is based on and can be applied to large-scale trajectory data. The utility of the model is demonstrated through a series of case studies using real aircraft trajectories.

1. Introduction

Safe operation of aircraft requires thorough understanding and persistent/routine monitoring of the risk between aircraft operating in the airspace. Many of the requirements and standards used for assessing risk internationally are mandated by organisations such as the International Civil Aviation Organisation (ICAO), with much of the original technical modelling undertaken by the Separation and Airspace Safety Panel (SASP). Member states then adopt the guidelines from ICAO as necessary, with the risk aspects typically delegated to Air Navigation Service Providers (ANSPs) or regulators. Thus, on a national level, ANSPs are responsible for reporting on safety and risk, including trends and underlying causes via a wide variety of airspace models.

There is a growing need for detailed monitoring and reporting of risk in domestic airspace, based on all recorded trajectories, i.e. for post-risk analysis. This will allow ANSPs to obtain detailed risk metrics giving a rich source of 'big data' to allow establishment of causes (and effects), hidden and emerging risks, and lead indicators for all conflicts, even for those that do not progress to a loss of separation (LOS). This requires a suitable model that is detailed enough to provide the necessary data, and scalable to apply to all aircraft traffic whilst still estimating risk in a meaningful way.

Typically, ANSPs conduct risk reporting via counts of occurrence types, for example, a time series of the number of LOSs. There are numerous models for conflict detection which could also be applied (see for example the review of Kuchar and Yang, 2000). These are broadly based around Air Traffic Control (ATC) short or medium term conflict detection tools, or aircraft-based Airborne Collision Avoidance Systems (ACASs). While these have metrics associated with the probability of a LOS, they are designed for tactical use as a True/False detection tool, rather than for post-risk analysis. Some ANSPs use ACAS alerts as a proxy model of risk events, but usually as a simple count (alert or not), rather than using the

(hidden) value of the alert parameter. Hence, conflict detection models are designed for tactical use, and not for post-analysis of risk and causal factors.

There has been a progression by ANSPs to improve the quantification of occurrence risk using subjective methods. Many ANSPs subjectively estimate the risk for each occurrence using risk assessment tools (RAT) or safety severity indices (Eurocontrol, 2015) or additional weightings (Kovacova et al., 2018). These are usually categorised as A to D or SSI 1 to 4 and based on estimates of closure rates, percentage LOS, time to closest point of approach (CPA), barrier models (barriers that failed to prevent the LOS and those that prevented a collision) and bow-tie methodologies. However, these models are time-consuming and rely on subjective assessments, and are not suited to massive 'large-data' analysis of thousands of conflict events.

Completely quantitative approaches provide a more consistent and verifiable means to assess risk across different airspaces, ANSPs and regulators. For separation standard development by ICAO, the Anderson model (Anderson and Lin, 1996; Anderson 2000a, 2000b, 2003, 2005) is used for same-identical and crossing tracks with additional work by Aldis and Barry (2015). For monitoring in simple airspace, mathematically aggregated collision risk can be used. Examples of these are lateral routes, vertical separation in reduced vertical separation minimum (RVSM) airspace (ICAO, 2019) and longitudinal separation in oceanic airspace (ICAO, 2017), where the latter model is based on Anderson's approach. These produce continuous mathematically based risk metrics from large volumes of surveillance data, allowing a direct measure of risk against agreed target levels of safety (TLS). These aggregated results are not on the level of individual aircraft encounters, so detailed analysis of causes and effects, for example, are not possible. Furthermore, they only apply to some simple structured airspaces such that complex domestic airspace cannot be modelled this way.

For more complex airspace, risk modelling needs to be done on a per encounter (or conflict) basis to meet ANSP reporting requirements. There has been previous work on conflict-based risk methods, for example, that by Netjasov (2012) and Arnaldo et al. (2012). Parker (2019) has recently proposed a metric based on a weighted formula, combining the time to closest point of approach (CPA), the loss of vertical separation and the loss of horizontal separation at the CPA. While simple and easily implemented, the model uses parameter values assessed by subject matter experts but without a strong mathematical foundation. Similarly, Arnaldo et al. (2012) looked at overlap models based on the CPA. Whilst the CPA is generally a reasonable approximation of the riskiest part of aircraft trajectories, it is only a static metric at a single point and does not consider the entire trajectories.

A clear solution to the quantitative large-scale monitoring of complex airspace is thus lacking. This paper presents a mathematically based collision risk model that quantifies the risk of all types of aircraft encounters such as a LOS or a conflict. The model provides a method of estimating risk that is efficient enough to be applied to large aircraft trajectory data sets to establish causes of risk, lead indicators and hot-spots among other important analysis. The contributions of this paper are as follows.

(a) A new model that extends earlier SASP approaches by combining key elements of the models by Aldis and Barry (2015) and Anderson (2005) to estimate collision risk for pairs of aircraft trajectories, whilst overcoming issues when applied to real trajectories including degenerate cases.
(b) New models for position uncertainty propagation that accounts for aircraft trajectory behaviour, as well as a new continuous time intervention model for domestic airspace with very high frequency (VHF) voice communications.
(c) Application of the proposed risk model to real case studies of aircraft conflicts, and a comparison to an existing approach.

This paper is structured as follows. Section 2 provides important background information on the Anderson (Anderson and Lin, 1996; Anderson, 2000a, 2005) and the Aldis models (Aldis and Barry, 2015) with added details of the timing and intervention model including supporting evidence. Section 3 develops a new model for aircraft encounters which combines the Aldis model and intervention model, with further adaptations to manage degenerative cases (specific geometries) and position uncertainty propagation. Section 4 provides multiple case studies from actual encounters to demonstrate how the

https://doi.org/10.1017/S0373463323000085 Published online by Cambridge University Press

results can be practically applied to real scenarios, as well as a comparison to a risk score from Parker (2019).

2. Background

The ICAO SASP have used a variety of modelling methods to define appropriate separation standards for an airspace. These are often divided into models for aircraft separated laterally, longitudinally or vertically and run on specific encounter geometries.

For lateral separation of aircraft routes in oceanic airspace, the models developed by Reich (1966a, 1966b) are used. These models define the probability of lateral overlap of two aircraft nominally located on adjacent tracks based on assumed distributions of lateral position. Initially, the approach did not include any communication model, with an implicit assumption that the cause for the lateral position distribution was some intervention to a deviation. Recently, these approaches incorporate space-based satellite surveillance (ADS-B, automatic dependent surveillance-broadcast) models (developed by SASP) which include a timing and intervention component. Such models better represent the real traffic scenario for these structured airspace regions. However, these models are not suitable for analysing specific aircraft trajectories, as they operate on aggregate populations of aircraft.

The evolution of ADS-B (broadcast surveillance data from an aircraft) and ADS-C (surveillance data sent to the controller via a satellite contract) allows for rich analysis of aircraft trajectories. Prior to the ADS environment, trajectory data were only available from radar and isolated within the ANSP. Since ADS data are of much higher accuracy than radar, with detailed uncertainty measures encoded within the message, there is no risk in using these data within the analysis. However, the goal of this paper is to propose a method for risk analysis, regardless of the data source used.

Modern oceanic operations are significantly different from domestic airspace. In remote and oceanic regions, the surveillance has usually been by ADS-C, with surveillance data only available at intervals defined by the satellite contract; these are usually at 10, 14 and 30 min intervals. Only with Aerion space-based ADS-B has more frequent surveillance been available. Communication is also slower, and usually by satellite using a method called CPDLC, with a third-party HF backup system. These communications must meet precise required communication performance (RCP). These communication methods have intervention times of the order of 4–14 min (Anderson, 2000a, 2000b, 2005). Oceanic traffic is also usually either on simple fixed route systems, such as the North Atlantic parallel track structure, or purely free-routing in areas of very low traffic density. In domestic airspace, fast VHF-voice communications allow for aircraft vectoring and aircraft in close proximity. Hence, the risk modelling for oceanic versus domestic airspace is quite different. For oceanic airspace, the risk monitoring can make assumptions regarding aircraft tracking and navigational performance, since the route structures are usually simpler. In domestic airspace, risk monitoring has been very difficult due to much more varied airspace tracking and vectoring, and hence has not been able to use the same detailed risk modelling.

For aircraft on intersecting tracks or for aircraft following each other (i.e. a same-identical track scenario), models based on reliability theory (Hsu, 1981) developed by Anderson (Anderson and Lin, 1996; Anderson, 2000a, 2005) are used. Anderson modelled the distribution of aircraft in the along and cross-track directions as first-Laplace (double exponential) distributions. At any point in time, the horizontal overlap of the two aircraft was calculated analytically. The equations were derived using computer algebra tools to perform the multiple integrals, generating 16 sets of equations representing the various combinations of the integral domain: the left and right components of the Laplace distribution, for each along and cross track positional deviations for both aircraft. The model then allowed the overlap probabilities to be integrated over any specified time-span to calculate an effective collision risk.[1] For example, when deriving 30 NM (and now 20 NM) oceanic separation standards (SASP), the risk was integrated over the projected paths for time up to $4 \cdot 0$, $10 \cdot 5$ and $13 \cdot 5$ min from the initial aircraft

[1]The Anderson derivation assumed the aircraft sizes were small with respect to the distribution scale. This is usually true with the scale parameter of the distribution usually related to the required navigation performance (RNP) value, ($\lambda \approx$ RNP/log 20) and hence having a value of the order of 1 NM, compared to an aircraft dimension of $0 \cdot 037$ NM (224 ft, 64 m).

https://doi.org/10.1017/S0373463323000085 Published online by Cambridge University Press

positions and orientations. These times were based on a model of controller–pilot intervention for oceanic airspace using satellite communications with HF-voice as a secondary communication means. This was repeated through a series of double integrals modelling the potential errors in forecast aircraft speed. The final model was then a series of multiple integrals over time, speed, aircraft initial positions and aircraft position error to find a collision risk value for any given separation. This gave the critical separation that made the risk less than the TLS.

The Anderson model can be used to estimate risk for any pair of crossing tracks, but when applied to aircraft on most angles (i.e. not 0°, 90° or 180°), the algorithm is very computationally expensive. The model was therefore simplified by Aldis and Barry (2015) by analytically integrating the tracks from $t = -\infty$ to ∞. However, this does not include any model for intervention time, since the overlap probabilities are calculated for the entire past and future extrapolated paths. This limitation can be overcome by applying the timing intervention model after calculation of the Aldis model, and by using the time between the current position and the CPA. This moves the timing intervention model outside the full Anderson integral, which makes no difference to the accuracy of the model but allows for several orders of magnitude improvements in computational speed.

The Aldis model is an adaptation of the well-established Anderson model, commonly used within SASP and by Australian and US ANSPs for monitoring risk. The model is typically used to assess risk of straight line crossing trajectories, for which it estimates the probability of collision. The model can however be extended to assess the risk of any pair of trajectories, linear or otherwise, based on linear projections which is the focus of this paper. These extensions require careful consideration of some relative geometries to ensure meaningful and representative risk estimates are obtained. Furthermore, modifications to other components of the Aldis model are needed to ensure the model still meaningfully estimates collision probabilities when adapted to arbitrary trajectories without over- or underestimating risk. These modifications will also be explored in this paper.

The combination of the Aldis model and an intervention model is a key part of the proposed model. As such, more detail on the background of these parts is provided in the rest of this section.

2.1. Intervention time model

The model presented here includes the time it takes for a controller to notice a problem, send a message to the aircraft and resolve the issue. This is called the *intervention* or action time and is denoted τ. This is modelled as either a discrete set of times and proportions (τ_i, p_i) or as a continuous distribution $f(\tau)$. Hence, a conflict projected 20 min in the future will have negligible risk, whereas a conflict 30 s in the future will allow insufficient time for intervention.

In oceanic airspace, with well-defined satellite communications (controller–pilot data link communications – CPDLC), the intervention times, p_i, τ_i, can be accurately modelled. These are based on event sequence diagrams representing documented and legal requirements for surveillance and communications: required surveillance performance (RSP) and required communication performance (RCP) (ICAO, 2013). For example, pilot response times are required to occur in 60 s 95% of the time and the actual communication technical performance (ACTP) is required to be completed in 120 s 95% of the time. With all the components considered, the intervention time was modelled with proportions $p = [0{\cdot}9025, 0{\cdot}4075, 0{\cdot}05]$ and times $\tau = [4, 10{\cdot}5, 13{\cdot}5]$ min (Anderson, 2000a, 2000b, 2005).

Within domestic airspace (with push-to-talk VHF communications), this intervention time is less well known, since the VHF communication system is not conducive to large-scale monitoring and deciphering. However, there are sufficient studies to make a reasonable intervention model (an exponential distribution starting at 45 s with a 45 s scale parameter) (Cardosi, 1993a, 1993b; Morrow et al., 1993; Prinzo, 1993; Burki-Cohen, 1995; Cardosi et al., 1995, 1997a, 1997b, 1998; Gonda et al., 2005; Prinzo and McClellan, 2005; Chen, 2010; Nickelson, 2018).

The ability of the controller to notice a conflict and intervene will vary according to many factors, including airspace complexity, workload, training and so on. This is taken into account by the distribution in the model. Hence, the longer tails of the distribution model situations where a controller is slower in

https://doi.org/10.1017/S0373463323000085 Published online by Cambridge University Press

resolving conflicts. Where appropriate, it is easy for an implementer of the model to change the currently used values of 45 s, in line with their airspace. This paper is not prescribing a particular intervention distribution, but demonstrating how the risk model can be used with a reasonable intervention model. Other distributions for the intervention model can be used without loss of generality.

The key components of the intervention times can be summarised as follows (with mean and standard deviation (st.dev) taken from Cardosi et al. (1995, 1997a, 1998) and Cardosi (1993a, 1993b). These are the times, in seconds:

- for the controller to notice a deviation and begin voice communications (≈15–30);
- for the controller to deliver the message (≈5–10, – mean $4 \cdot 8$, st.dev $2 \cdot 3$);
- between the controller ending the message and the pilot initiating a response (mean $3 \cdot 3$, st.dev $4 \cdot 8$);
- for the pilot to talk (mean $2 \cdot 6$, st.dev $1 \cdot 8$);
- for possible readback errors, miscommunications and repeating of instructions (of the order of 1–3% of communications: Morrow et al., 1993; Cardosi et al., 1997a);
- for the pilot to initiate a manoeuvre (≈2–5);
- for the aircraft to deviate to avoid the conflict (≈15–75).

The Cardosi papers indicate a total communication time (not including the aircraft manoeuvring) of (9, 17, 23, 40) s with cumulative percentiles (50%, 90%, 95%, 99%). Cardosi noted that the times from the controller initiating communications to the final speed acknowledgement had a mean of 18 s with a range between 3 and 71 s. This study also noted the pilot response times having a mean of $10 \cdot 8$ s, (minimum 4, maximum 40 s, st.dev $5 \cdot 9$ s) and percentiles (5, 10, 50, 90, 95)% in (5, 6, 9, 17, $22 \cdot 5$) s.

An analysis of terminal operations gave results for 'pilot–controller discourse' with mean 20 s and st.dev 5 s (Rantanen et al., 2004). Recent SASP work (Nickelson, 2018) noted communication times of $3 \cdot 6$–$6 \cdot 3$ s, and the time for the aircraft to start a trajectory change (16 s, st.dev 10 s, 95% in 30 s). This paper noted a response climb rate of $4 \cdot 1$ s (95% in $9 \cdot 6$ s) per 100 ft, giving a time to clearance (500 ft) of the order of 21–48 s.

In summary, the modelling of intervention time in a VHF-voice environment is hence not precise compared to oceanic airspace, with a moderate range of values reported in the literature. Here, we use a simple exponential distribution with scale factor and location both 45 s (further mathematical description in Section 3.1). Hence, no intervention is possible within 45 s of a deviation, and 50% of deviations would be fully resolved within 90 s: these values include the full intervention time, from an aircraft beginning to deviate, through to the aircraft manoeuvring to be safely separated. While it is possible to generate more exotic distributions, such as a Gamma, the exponential distribution is simple and is long-tailed, allowing for known occurrences where controllers do not detect the conflict, because pilot–controller communications are inadequate or because pilot responses are incorrect.

2.2. Aldis model

The Aldis model is a variation of the Anderson model in which the temporal integral limits become infinite (Aldis and Barry, 2015). Here, we disregard the uncertainty on the velocities of the two aircraft and the separation distance, which speeds up calculations significantly by removing three integrals. Typically, these integrals would be used for strategic evaluation of collision risk to account for the probability distributions of the speeds of all aircraft at the crossing, as well as the distribution of possible separation distances between pairs of aircraft. However, the adaptations made to use the model for evaluating aircraft encounters based on data means that the velocities of the two aircraft at each position are known, as well as their separation in terms of a crossing track projection, and as such these uncertainties are discarded.

The collision risk for two aircraft on two infinitely long crossing tracks is given by

$$\mathrm{CR}^{\infty} = N_p \int_{-\infty}^{\infty} \mathrm{HOP}(t \mid V_1, V_2)\ P_z(h_z) \left(\frac{2V_r}{\pi \lambda_{xy}} + \frac{\overline{|\dot{z}|}}{2\lambda_z} \right) dt, \tag{2.1}$$

https://doi.org/10.1017/S0373463323000085 Published online by Cambridge University Press

with V_1, V_2 the speeds of both aircraft, $|\dot{z}|$ the mean relative vertical speed (usually considered $1 \cdot 5$ knots for aircraft on the same flight level), V_r is the relative speed between the aircraft, h_z is the vertical separation, P_z is the vertical overlap probability, N_p is the number of pairs per flight hour, λ_{xy} is the mean aircraft horizontal size, λ_z is the aircraft mean vertical size and the horizontal overlap probability is denoted HOP. The last terms in the brackets are often called the kinematic terms.

Denote the initial distances of the two aircraft from the intersection point d_{10} and d_{20}. The horizontal overlap probability is then given by

$$\begin{aligned}\text{HOP} = 2\pi\lambda_{xy}^2 \int_{-\infty}^{\infty}\int_{-\infty}^{\infty} [f_2^A(\xi)\, f_2^C(\eta)\, f_1^A(\xi\cos\theta - \eta\sin\theta - D_x(t)) \\ \cdot f_1^C(\xi\sin\theta + \eta\cos\theta - D_y(t))]\, d\xi\, d\eta,\end{aligned} \tag{2.2}$$

where θ is the angle between the aircraft tracks, the functions $f(\cdot)$ are the position uncertainty distributions in the along and cross-track directions for aircraft 1 and 2, and

$$\begin{aligned}D_x(t) &= (V_1 - V_2\cos\theta)t - d_{10} + d_{20}\cos\theta, \\ D_y(t) &= (d_{20} - V_2 t)\sin\theta.\end{aligned}$$

Equation (2.2) calculates the horizontal overlap probability by convolving the two position error densities of the two aircraft to find the density describing their separation. The density of one aircraft needs to be rotated and shifted so that it is in the coordinate reference frame of the other aircraft. The probability of overlap can then be found from the separation density by integrating over the area of the two aircraft around the origin, i.e. capturing the probability of the separation being less than the combined aircraft dimensions which defines a collision. To simplify this calculation, rather than integrating the result of the 2D convolution, the result is evaluated at zero and multiplied by the area of the two aircraft to approximate the probability of collision.

It is assumed that the kinematic terms and the vertical overlap probability in Equation (2.1) are constant, which allows evaluating them outside the integral. The order of the time t and space integrals ξ and η can be reversed, which yields

$$\text{CR}^{\infty} = 2N_P \left(\frac{2V_r}{\pi\lambda_{xy}} + \frac{\overline{|\dot{z}|}}{2\lambda_z}\right) P_z(h_z) I_1^*, \tag{2.3}$$

$$I_1^*(V_1, V_2) = \pi\lambda_{xy}^2 \int_{-\infty}^{\infty}\int_{-\infty}^{\infty} f_2^A(\xi)\, f_2^C(\eta) I_2^*(\xi, \eta \mid V_1, V_2)\, d\xi\, d\eta, \tag{2.4}$$

$$I_2^*(\xi, \eta \mid V_1, V_2) = \int_{-\infty}^{\infty} f_1^A(\xi\cos\theta - \eta\sin\theta - D_x(t))\, f_1^C(\xi\sin\theta + \eta\cos\theta - D_y(t))\, dt, \tag{2.5}$$

where f_1^A and f_2^A are the along-track position errors, and f_1^C and f_2^C are the cross-track errors of the two aircraft. The term $I_1^*(V_1, V_2)$ is the horizontal overlap probability for the infinitely long tracks, and once multiplied by the vertical overlap probability and the kinematic terms in Equation (2.3) will yield the collision risk.

The time integral can be further simplified. It is assumed that the along and cross track position errors of both aircraft are Laplace distributed with scale parameters λ and ν, and noting that the initial distance of aircraft 2 $d_{20} = 0$,

$$I_2^*(\xi, \eta \mid V_1, V_2) = \frac{1}{4\lambda\nu} \int_{-\infty}^{\infty} e^{-|\alpha|\cdot|a/\alpha + t|}\, e^{-\beta|b/\beta + t|}\, dt, \tag{2.6}$$

https://doi.org/10.1017/S0373463323000085 Published online by Cambridge University Press

where

$$\begin{aligned} a &= (\xi \cos\theta - \eta \sin\theta + d)/\lambda, \\ b &= (\xi \sin\theta + \eta \cos\theta)/\nu, \\ \alpha &= (V_2 \cos\theta - V_1)/\lambda, \\ \beta &= V_2 \sin\theta/\nu, \\ d &= d_{10} - V_2 d_{20}/V_1. \end{aligned} \tag{2.7}$$

The parameters α and β do not depend on ξ or η. Note that the angles 0 and π are excluded which, along with $V_2 \neq 0$, mean that β is strictly positive. The parameter α can however have either sign.

The substitution of a new time variable $u = a/\alpha + t$ into Equation (2.6) results in

$$I_2^*(\xi, \eta \mid V_1, V_2) = \frac{1}{4\lambda\nu} \int_{-\infty}^{\infty} e^{-|\alpha|\cdot|u|}\, e^{-\beta|\zeta+u|}\, du, \tag{2.8}$$

where

$$\begin{aligned} \zeta &= \frac{b}{\beta} - \frac{a}{\alpha} \\ &= -\frac{V_1}{V_2(V_2\cos\theta - V_1)}\xi + \frac{V_2 - V_1\cos\theta}{V_2 \sin\theta (V_2\cos\theta - V_1)}\eta - \frac{d}{V_2\cos\theta - V_1}, \end{aligned} \tag{2.9}$$

and thus ζ is linear in ξ and η.

The time integral in Equation (2.8) can now be evaluated to give

$$I_2^*(\xi, \eta \mid V_1, V_2) = \frac{1}{2\lambda\nu(\alpha^2 - \beta^2)}(|\alpha|\, e^{-\beta|\zeta|} - \beta\, e^{-|\alpha||\zeta|}). \tag{2.10}$$

Two special cases also exist. If $\alpha = 0$, the x-distance between the aircraft is constant, and the integral evaluates to

$$I_2^*(\xi, \eta \mid V_1, V_2) = \frac{1}{4\lambda\nu} \int_{-\infty}^{\infty} e^{-|a|}\, e^{-|b+\beta t|}\, dt = \frac{e^{-|a|}}{2\beta\lambda\nu}. \tag{2.11}$$

If $\beta = |\alpha|$, two identical Laplace distributions are convolved, which simplifies the integral to

$$I_2^*(\xi, \eta \mid V_1, V_2) = \frac{1}{4\lambda\nu} \int_{-\infty}^{\infty} e^{-|a+\alpha t|}\, e^{-|b+|\alpha| t|}\, dt = \frac{1}{4\lambda\nu} e^{-\beta|\zeta|} \left(|\zeta| + \frac{1}{\beta}\right). \tag{2.12}$$

The spatial integral in Equation (2.4) can now be evaluated using a time integral in Equations (2.10), (2.11) or (2.12) as appropriate, and the solution used to calculate the collision risk with Equation (2.3). The analytical solutions to Equation (2.4) are reported by Aldis and Barry (2015).

The Aldis model has been numerically tested against the Anderson model and found to accurately represent the integration over infinite time. Some special cases however will be discussed further in Section 3.4.

3. Model development

This section considers the development of a new model based on the Aldis model that applies to arbitrary aircraft trajectories. Consider two aircraft whose trajectories are denoted by $X_1(t)$ and $X_2(t)$, respectively. The trajectories are known completely, i.e. the analysis is conducted on historical data. For two aircraft which did not collide, the goal is to estimate the risk at each time point if no intervention had occurred: a scenario which simulates the case of 'what-if interventions had failed' (how close were the aircraft to a collision).

https://doi.org/10.1017/S0373463323000085 Published online by Cambridge University Press

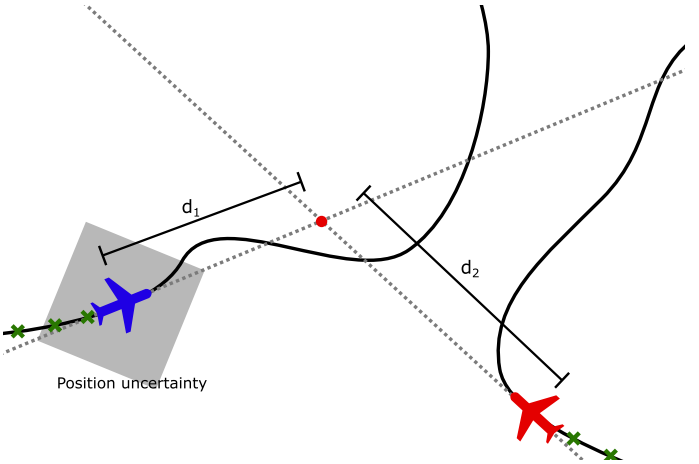

Figure 1. *Application of the Aldis model to aircraft trajectories. Two aircraft are shown at a snapshot in time along their known trajectories. The dotted lines are infinite length projections of their paths from a given time point. The red dot identifies their crossing point. The two aircraft are a distance of d_1 and d_2 from the crossing point, respectively.*

The risk of collision between the two aircraft as a result of their respective trajectories is estimated at each time step t_i by projecting straight-line trajectories from the current positions of the two aircraft, as shown in Figure 1. Note that these projections extend infinitely in front and behind the aircraft to allow the use of the Aldis model for fast evaluation of the collision risk, as described in Section 2.2 by incorporating the position uncertainty of both aircraft. The time to the CPA or conflict is incorporated by later inclusion of the time intervention model.

Hence, a risk value is determined for all time steps, $R_i \equiv R(t_i)$, conditional on the aircraft flying a straight-line path. This means the overall risk is not an integration of R_i because of the conditionals for which probabilities are not known, but instead the maximum value of R_i corresponding to the point in time where the projected crossing track configuration generated the highest risk of collision.

The details of the model are further described in the following subsections, which discuss how controller intervention, aircraft position uncertainty and vertical overlap probability are modelled. Finally, the treatment of degenerate cases is explained.

3.1. Intervention model

The collision risk model includes a component that tries to model the time taken for an air traffic controller to notice an impending collision and intervene. In particular, the probability of the controller failing to intervene is modelled by a shifted exponential distribution over time $E(\mu, \lambda)$ with location $\mu = 45$ s and scale $\lambda = 45$s. If the time to CPA is less than the mean μ, the probability of no intervention is set to 1 (the probability of intervention is 0). Thus, the probability of no intervention $P(\bar{I})$ is given by the piece-wise equation, where τ is the time to the CPA,

$$P(\bar{I}) = \begin{cases} e^{(\mu-\tau)/\lambda} & \tau > = \mu, \\ 1 & \tau < \mu. \end{cases} \tag{3.1}$$

The Aldis model does not account for the time to CPA and intervention time model. By post-multiplying the Aldis model risk by Equation (3.1) however, based on the time to CPA, we can approximate the use of the Anderson model with a time integral based on the intervention time distribution.

https://doi.org/10.1017/S0373463323000085 Published online by Cambridge University Press

3.2. Aircraft position uncertainty

Traditionally, the Anderson model is applied to determining the strategic collision risk at intersections of aircraft traffic. In these cases, the aircraft tracks are predetermined, and the position uncertainty of the aircraft travelling on them is described by the required navigation performance (RNP) of the routes (ICAO, 2008). In particular, the Laplace distributions used for the lateral and longitudinal navigation performance have their scale parameter λ derived from the RNP values, such that

$$\lambda = \frac{\text{RNP}}{\log 20}. \tag{3.2}$$

The RNP value is part of performance based navigation (PBN) specifications with an engineering and legal requirement on an aircraft's ability to maintain a track line. The value (i.e. RNP 4) relates to 95% containment of the aircraft position within 4 NM of the centre-line along with an on-board alerting ability. In practice, the navigation performance of aircraft is significantly better, which is described by observed navigation performance (ONP). For example, aircraft with RNP 4 NM often perform with ONP equivalent to $0 \cdot 02$ NM. Hence, for risk calculations to be conservative, they are done using both the legal RNP level and an ONP level, since both can be appropriate in different circumstances.

In the context of this paper, neither RNP nor ONP is appropriate however, because at each time step, the crossing aircraft tracks are extrapolated from the current known positions of each aircraft. As a result, each aircraft is by definition known to be at the centre of its track at the start, which is at odds with the typical strategic model that assumes steady-state behaviour. Therefore, at that time step, the position error of each aircraft relative to the projected track is near zero, and it must grow over time. The small level of surveillance inaccuracy in the recorded position can be discounted.

It is proposed that the position uncertainty of the aircraft both in the lateral and longitudinal directions is modelled by a random walk, of the form:

$$X_t = X_{t-1} + \epsilon_t, \tag{3.3}$$

$$X_0 = 0, \tag{3.4}$$

where X_t is the position of the aircraft at time t for the projected track and ϵ_t is a step that is chosen from a probability distribution. Here, X_t has a variance of $t\sigma_\epsilon^2$ at time t, where σ_ϵ^2 is the variance of ϵ. Thus, the variance of X_t grows linearly as a function of t.

The distribution of X_t is assumed to be Laplace, as this is the assumption also used in the Aldis model. Its scale parameter can be found by equating the variance of a Laplace distribution with the variance of the random walk and solving for the scale parameter:

$$\begin{aligned} 2\lambda^2 &= t\sigma_\epsilon^2 \\ \lambda &= \sqrt{\frac{t}{2}}\sigma_\epsilon. \end{aligned} \tag{3.5}$$

The scale parameter of the aircraft's position uncertainty cannot however grow unbounded. After some threshold time t_l, the uncertainty is assumed to reach the ONP of the aircraft. Thus, the value of σ_ϵ is determined such that at time t_l, the value of λ reaches that given by the ONP. This implies that the aircraft will deviate randomly from its starting location, and given a long enough time, will converge to the ONP distribution, i.e. its position will be independent of where it started. As such, the scale parameter λ used in this paper is defined by

$$\lambda = \begin{cases} \sqrt{\frac{t}{2}}\sigma_\epsilon & 0 \le t < t_l, \\ \dfrac{\text{ONP}}{\log(20)} & t \ge t_l, \end{cases} \tag{3.6}$$

https://doi.org/10.1017/S0373463323000085 Published online by Cambridge University Press

where

$$\sigma_\epsilon = \frac{\text{ONP}}{\log(20)\sqrt{0 \cdot 5 t_l}}. \tag{3.7}$$

The analytical versions of the Aldis model assume that the scale parameter of the position uncertainty of the aircraft is constant. As such, for the projected trajectories, the scale parameter in each case is a constant determined using the time to CPA from where the trajectory projection is initiated.

3.3. Vertical overlap probability

The vertical overlap probability in the Aldis model is assumed to be constant and equivalent to the extrapolated vertical separation at the CPA (based on climb and descent rates of the aircraft if appropriate). The rate of change of the difference in altitude of the two aircraft is set to zero if it is less than 100 ft/min, as this is generally indicative of errors in the altitude data rather than a clear climb or descent, which are usually of the order of 1000 ft/min.

If the two aircraft cross vertically during the projection, the extrapolated separation is conservatively set to zero. For example, consider one aircraft at 35,000 ft, the other climbing from 34,000 ft at 1000 ft/min and a CPA that is 2-min away. One might assume that at the CPA, the aircraft will then be safely at 35,000 and 36,000 ft. However, there is no guarantee that the climbing aircraft will not stop climbing at 35,000 ft (indeed this will often occur). Hence, to account for these situations, if the extrapolated vertical separation crosses zero feet, then it is set to zero.

The vertical overlap probability is calculated by assuming Laplace distributions for the altitude error of both aircraft, resulting in

$$P_z(h_z) = \int_{-\lambda_z}^{\lambda_z} \int_{-\infty}^{\infty} f(z_1)\, f(h_z + z_1 - z)\, dz_1\, dz, \tag{3.8}$$

where $f(\cdot)$ is the probability density function of a Laplace distribution. The scale parameter of this distribution is 38 ft, unless the mean altitude of the encounter is in non-RVSM airspace, in which case it is doubled to 76 ft.

3.4. Degenerate cases

The Aldis model becomes impractical at angles near 0° or 180°. As mentioned in Section 2.2, the Aldis model is strictly not defined for angles exactly equal to 0° or 180°. Additionally, the Aldis model also diverges from the Anderson model by overestimating collision risk at angles close to 0°, as the aircraft pair stays in close proximity for an increasingly longer time. This results in the I_1 integral increasing without bound as the angle between the aircraft drops to zero, especially if the two aircraft are flying at the same speed.

For these degenerate cases, the Anderson model must be employed. In general, the Anderson model is very computationally expensive; however, the angles of 0°, 90° and 180° are simple analytical formulations. The Anderson model requires bounds on the time integral, which must be set. The integral is evaluated from 0 to 4 min; for cases where the actual time to CPA is greater than 4 min, the probability of intervention by ATC is extremely high and the collision risk would be negligible anyway. Therefore, for crossing track angles less than $2 \cdot 5°$, the Anderson model is employed using an angle of 0°. The effect of this can be seen in Figure 2, where the dashed blue line represents the Aldis model for angles greater than $2 \cdot 5°$, and for smaller angles, the Anderson model evaluated at $\theta = 0$ is used. The plot shows that the result remains conservative, as the Aldis model overestimates the risk given by the Anderson model. For crossing angles closer than 1° to 180°, the Anderson model is also used, this time evaluated at $\theta = 180$.

https://doi.org/10.1017/S0373463323000085 Published online by Cambridge University Press

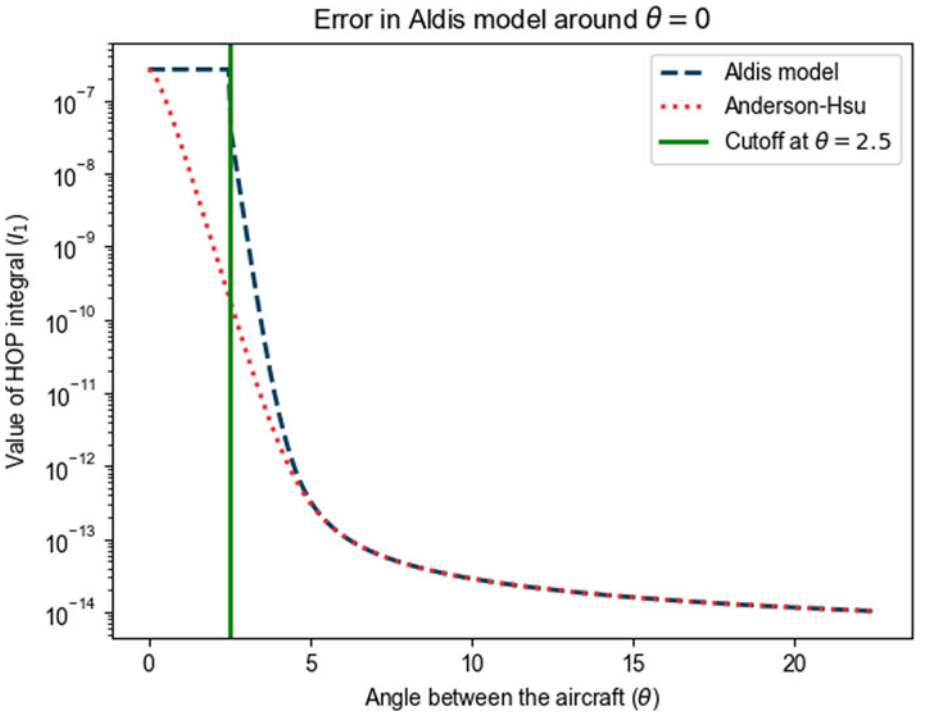

Figure 2. *Comparison between the standard Anderson model and the infinite track variation (Aldis) around a relative angle of zero. The Aldis model becomes more inaccurate (conservatively over-estimating the risk) near angle 0, and can be replaced by the Anderson model with default 0°.*

4. Model validation

This section applies the presented model to real aircraft encounter data. Three example encounters are analysed to show how the risk is evaluated in each case. The de-identified trajectories are based on ADS-B surveillance data which have been smoothed and interpolated to 5-s intervals.

4.1. Classical case

The first case concerns two aircraft heading towards each other, as well as converging towards the same flight level, as can be seen in Figure 3. The aircraft icons are plotted every minute. In the top left plot, the black aircraft highlight the location where the aircraft were closest to each other, and the top right and middle plots highlight the time and position of maximum risk. The closest approach and the maximum risk occurred at very different times, as at the point of closest approach, the two aircraft are already pointing away from each other and thus are not likely to collide, whereas at the point of maximum risk, they are projected to come much closer to a collision. The bottom plot shows the trajectory of the horizontal separation on the x axis and the vertical separation on the y axis over time. The red arrow indicates the projection of the separation of the two aircraft, with the red square at the end denoting the projected minimum separation of the two aircraft from the point of highest risk (blue square). It can be seen that the aircraft were projected to likely collide had they continued along this straight-line trajectory.

Figure 3 clearly shows the intervention, with aircraft AC 1 initiating a climb and lateral deviation, while AC 2 descends and deviates slightly. The figure also shows that the two aircraft barely avoided a LOS (5 NM, 1000 ft), indicated by the green rectangle on the bottom plot. However, the projected risk is high and if intervention had been delayed, the encounter may have been more significant.

https://doi.org/10.1017/S0373463323000085 Published online by Cambridge University Press

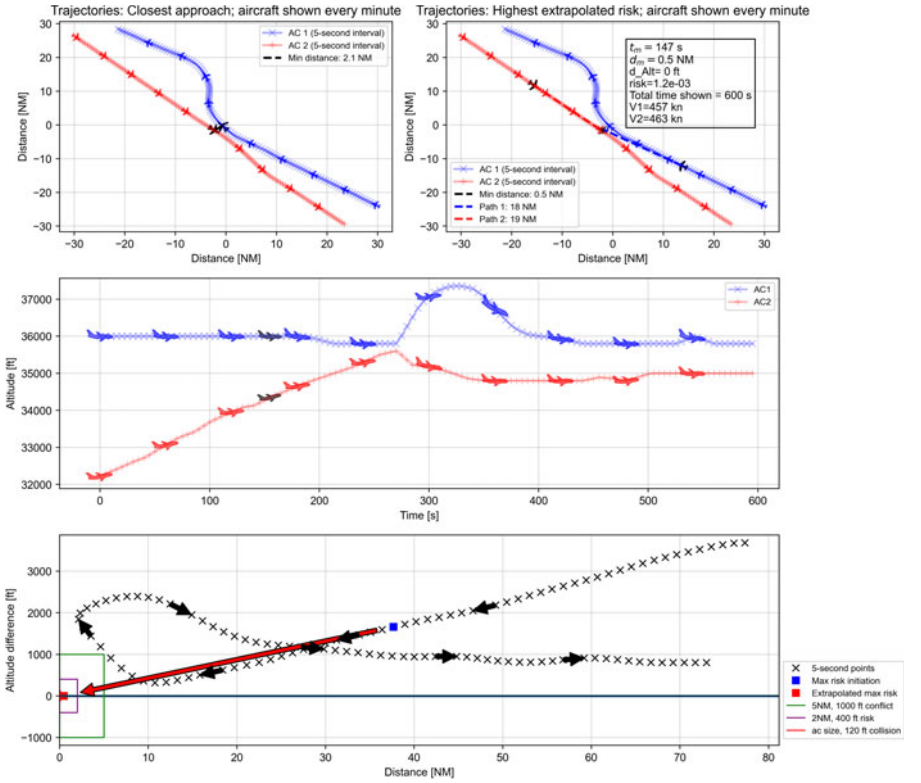

Figure 3. *Trajectory of the two aircraft in the first case. Top left is the trajectory with the point of closest approach highlighted by the black aircraft icons. Top right is the trajectory with the point of maximum risk highlighted by the black aircraft icons. The middle plot is the altitude over time, with the dark aircraft showing the point of maximum risk, and the bottom plot shows the trajectory of horizontal separation distance on the x axis and the altitude separation in the y axis. The aircraft icons and arrows are every minute, with the x every 5 s.*

4.2. Midair collision case

The second case was examined based on an actual midair collision between two aircraft. For confidentiality reasons, the aircraft trajectories cannot be shown. This case was considered to ensure that the model is able to accurately represent high-risk encounters.

A plot of the collision risk over time calculated by the model is shown in Figure 4 with different methods for estimating position uncertainty: the green line shows the random walk model used here, correctly having a risk that tends to 1. The blue line uses a position uncertainty based on the formal definition of RNP (4 NM). This RNP underestimates the risk, since two aircraft exactly aligned may still be 4 NM apart: whilst a reasonable assumption for modelling some separation standards, this is a poor model for modelling actual trajectory risk. The red line assumes a more realistic ONP model $0 \cdot 5$ NM, but still underestimates the risk close to the conflict.

The components of the collision risk using the proposed random walk approach are shown in Figure 5. The top plot shows the overall probability of collision trending correctly towards 1 (as these aircraft did collide). The second plot shows the horizontal overlap probability (also trending to 1). The third plot shows the vertical overlap probability, which has a maximum of $0 \cdot 55$ since altimetry errors mean two aircraft at the same level may still not be overlapping vertically. The bottom graph illustrates the probability of no intervention, which indicates no chance for intervention from approximately 250 s into the encounter.

https://doi.org/10.1017/S0373463323000085 Published online by Cambridge University Press

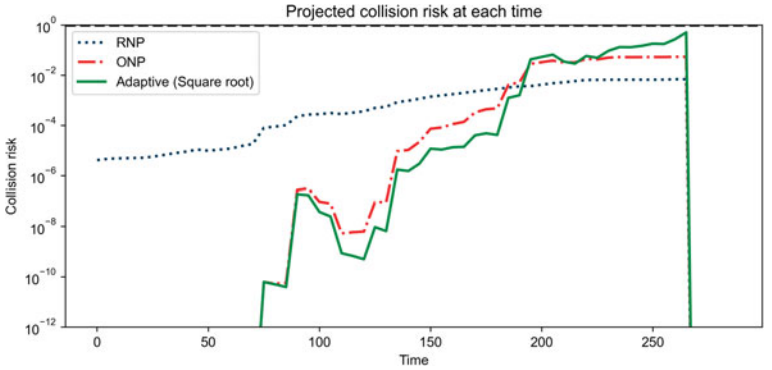

Figure 4. *Collision risk over time for the midair collision case. Plotted are the collision risk estimates at each time using three different notions of the position uncertainty. The dashed horizontal line represents a collision risk of 1.*

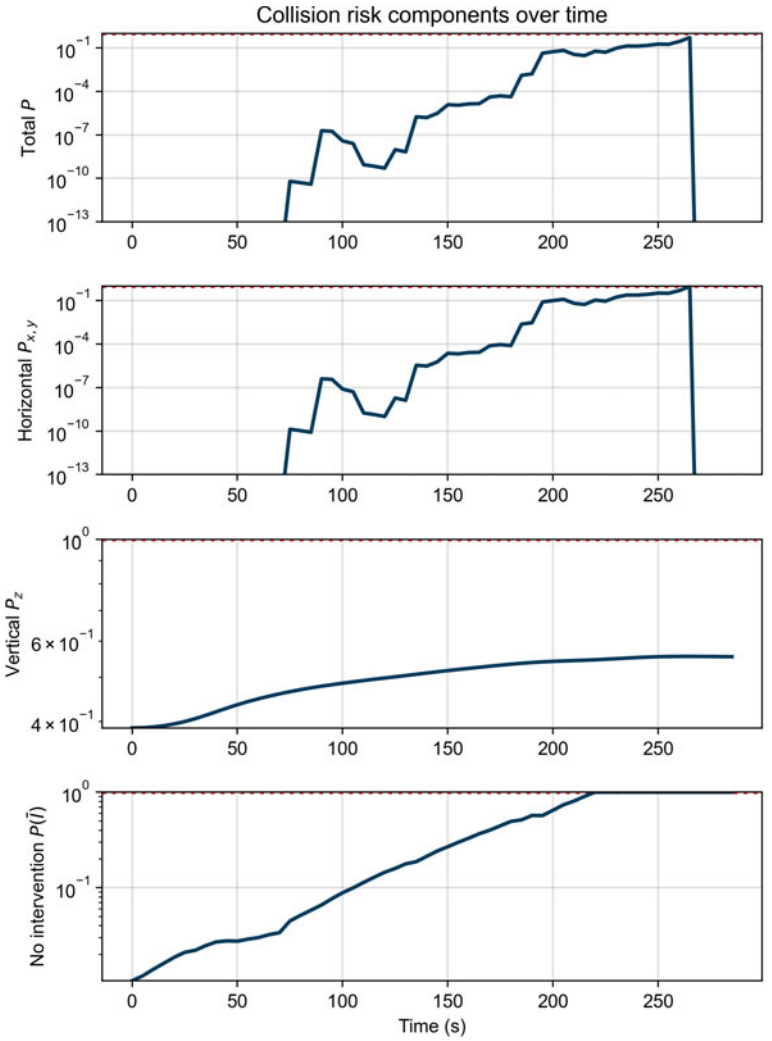

Figure 5. *Midair collision case. Projected risk is plotted at each time, along with its constituent multiplicative components. The red dotted line identifies a probability of 1.*

https://doi.org/10.1017/S0373463323000085 Published online by Cambridge University Press

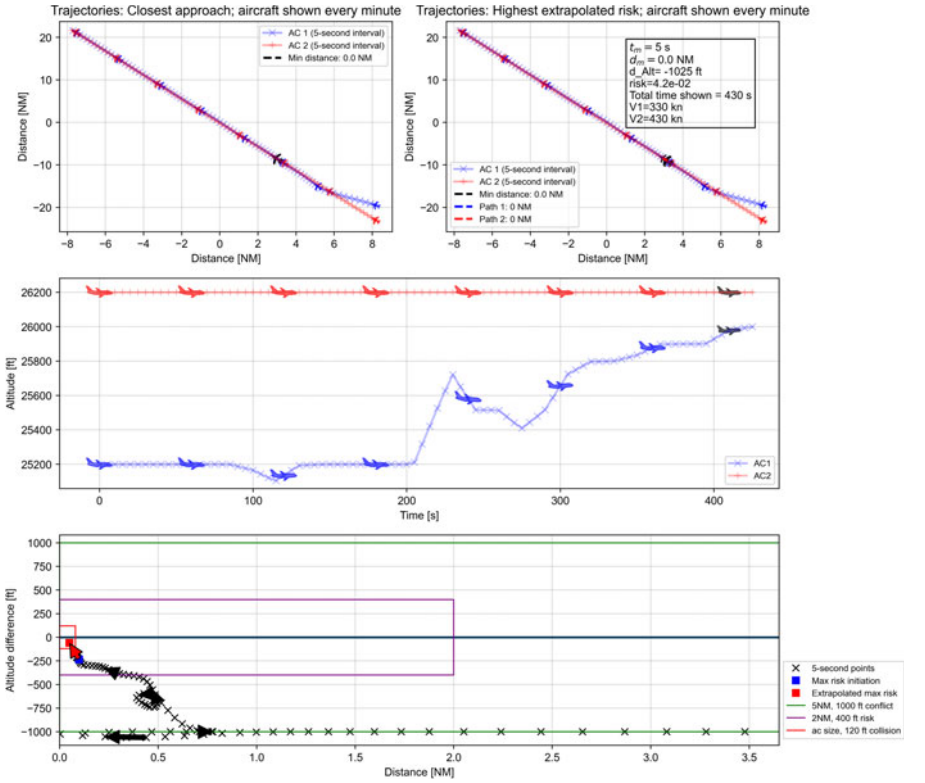

Figure 6. *Trajectory of the two aircraft in the same track case. Top left is the trajectory with the point of closest approach highlighted by the black aircraft icons. Top right is the trajectory with the point of maximum risk highlighted by the black aircraft icons. The middle plot is the altitude over time, with the dark aircraft showing the point of maximum risk, and the bottom plot shows the trajectory of horizontal separation distance on the x axis and the altitude separation in the y axis.*

4.3. Same track case

This case concerns two aircraft converging onto the same track, with one climbing to the flight level of the other aircraft, complicated by the difference in aircraft speeds (330 and 430 knots). The trajectories of the two aircraft are shown in Figure 6. The two aircraft merge onto the same track in the horizontal plane, but at different altitudes. The point of maximum risk then occurs around 220 s into the encounter, when the first aircraft starts climbing sharply, and its projected track is set to come very close to colliding with the second aircraft. The bottom plot shows that the projected tracks of the two aircraft at the point of highest risk will cause the two aircraft to overlap both horizontally and vertically if position error were completely neglected (shown by the red arrow that points into the small aircraft bounds box).

The collision risk components over time are given in Figure 7 showing that the collision risk evaluation between approximately 125–175 s and 250–290 s drops to be negligible. This drop is due to the velocity profile of the two aircraft in the horizontal plane, along with moments of descent, with the aircraft alternating places as the lead and follower aircraft due to the climbing behaviour of the first (blue) aircraft. In these time periods, the leader aircraft has a significantly higher speed and, as such, the two aircraft will never cross, meaning the risk evaluated is negligibly small. The risk of the entire encounter is evaluated by the maximum value, meaning these portions do not affect the overall evaluation of these types of encounters.

https://doi.org/10.1017/S0373463323000085 Published online by Cambridge University Press

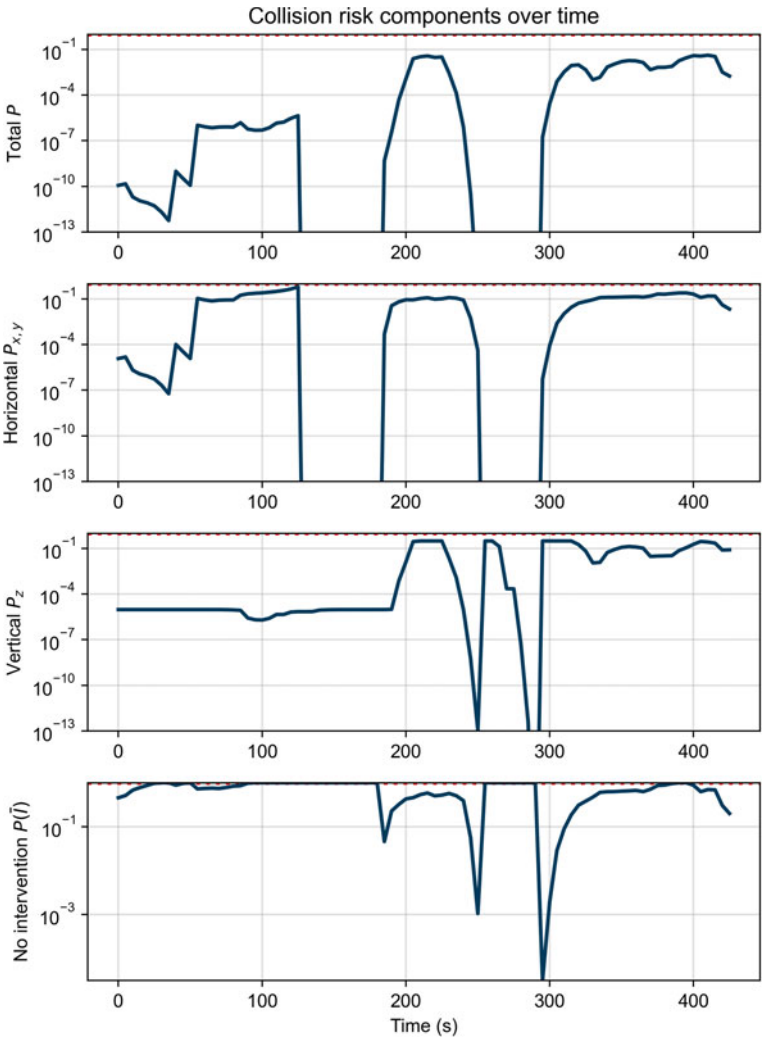

Figure 7. *Same track case. Projected risk is plotted at each time, along with its constituent multiplicative components. The red dotted line identifies a probability of 1. The risk drops to negligible levels during two periods, due to changes in speed and where the aircraft stopped climbing.*

5. Metric comparisons

An alternative metric for evaluating the risk of aircraft encounters is known as the MITRE score (Parker, 2019). It yields a risk score for straight-line trajectories of two aircraft, and is intended to be applied at each point of the trajectories of a pair of aircraft. The MITRE score is calculated using the three values of dT (time to CPA), dL (horizontal or lateral separation at CPA), dV (vertical separation at CPA):

$$\text{score} = \left(\frac{dT}{a}\right)^2 + \sqrt{\left(\frac{dL}{b}\right)^{2{\cdot}5} + \left(\frac{dV}{c}\right)^{2{\cdot}5}}. \tag{5.1}$$

The constants $a = 30$ s, $b = 0{\cdot}25$ NM and $c = 250$ ft are normalising constants. A comparison between the MITRE score and the model proposed in this paper is shown in Figure 8 for fifteen example encounters.

https://doi.org/10.1017/S0373463323000085 Published online by Cambridge University Press

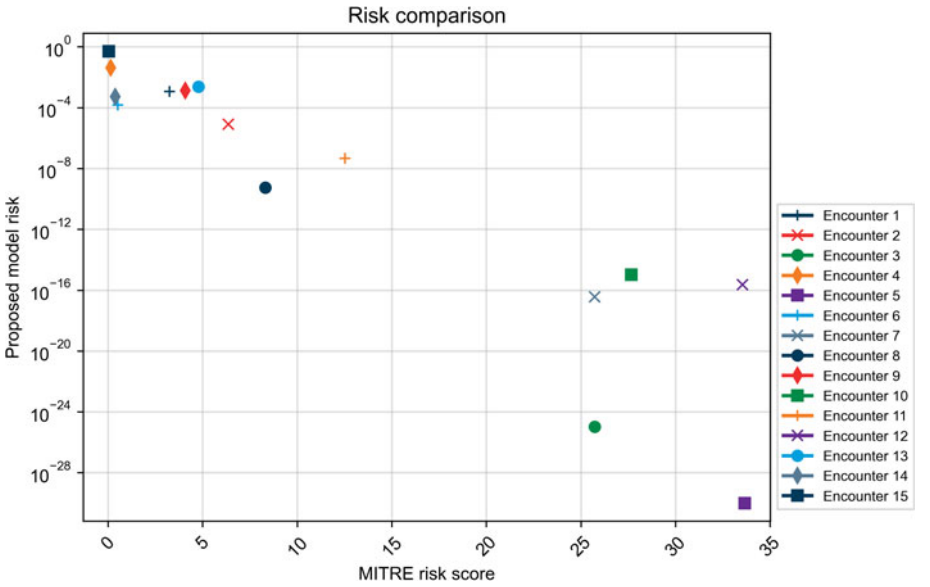

Figure 8. *Comparison between the proposed model risk on the y axis and the MITRE score metric on the x axis for various aircraft encounters. Smaller values for the MITRE scores signify more risk, whereas for the proposed model, larger values correspond to more risk. As expected, there is broad agreement (negative correlation) between the two metrics. Encounter 12 is explored further in Figure 9.*

An example of an outlier is Encounter 12, where the proposed approach rates as relatively more risky than the MITRE score, even though both approaches consider the same instance in time to be the riskiest. A plot of this encounter is shown in Figure 9. One reason for the difference is that at the CPA, the aircraft have a vertical separation, giving a small risk in the MITRE model. However, as in our calculations, the extrapolated vertical separation is zero, since the red aircraft may have descended to the flight level of the blue aircraft and then remained at that flight level, rather than crossing it.

6. Discussion

The proposed model attempts to directly estimate the collision probability between two aircraft on arbitrary trajectories. As the estimate is a probability, it is easy to both understand and use for classifying encounter risk. Furthermore, it can therefore be easily compared to risks calculated via other such models where appropriate (e.g. Reich model, Anderson model). Some other models, e.g. the MITRE model, cannot easily be used for this purpose, because risk scores are a relative measure which is only meaningful to the specific model that is used.

A further benefit of the model is that it applies to any arbitrary trajectories for the two aircraft. This includes movement in three dimensions, where altitude changes are treated with respect to actual aircraft behaviour. Degenerate cases which arise in the Aldis model are also handled, such that the model is readily applicable to all large-scale aircraft trajectory data. For some airspace, it may be necessary to use a different intervention model from that presented in this paper. For example, in airspace where CPDLC is dominant, a discrete model such as that in oceanic environments (Anderson, 2000a, 2000b, 2005) can instead be used to replace the intervention probability density function for more accurate risk estimates. In this way, the model is flexible and agnostic to the airspace and aircraft trajectories.

The main downside of the proposed model is that it assumes straight-line propagation of aircraft from each point, which is shared by most models of this type. As a result, these models are not as well suited to aircraft types that do not necessarily behave in this way, e.g. helicopters which can hover in place and do not necessarily need to continuously travel in a direction. This issue is fortunately somewhat

https://doi.org/10.1017/S0373463323000085 Published online by Cambridge University Press

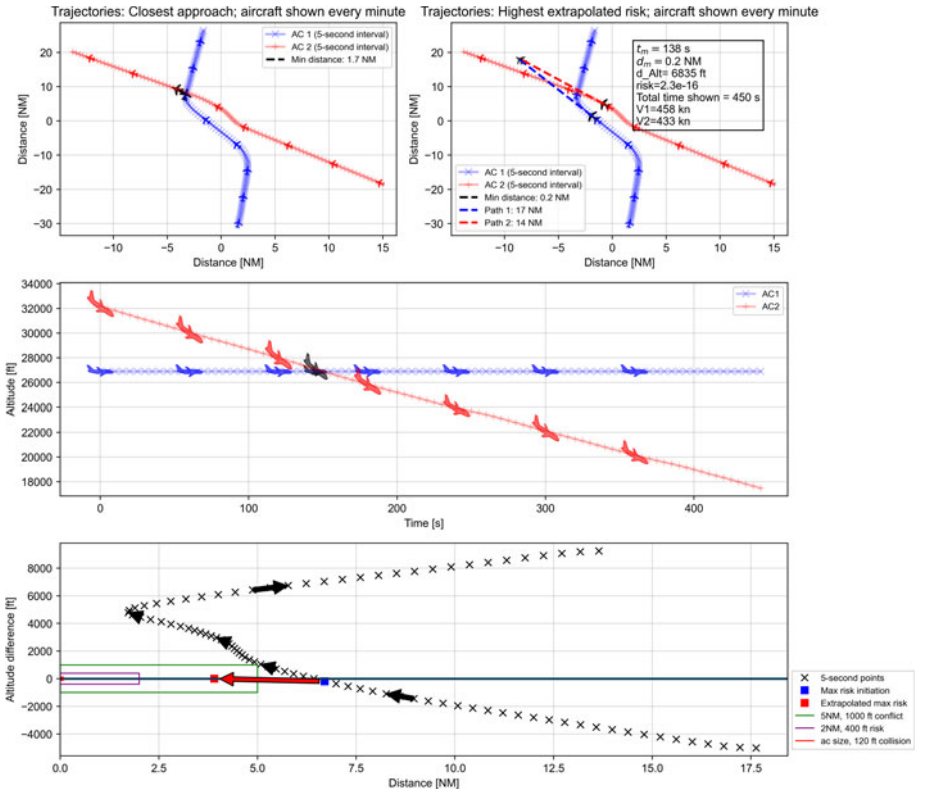

Figure 9. *Trajectory of the two aircraft in Encounter 12 from Figure 8. Top left is the trajectory with the point of closest approach highlighted by the black aircraft icons. Top right is the trajectory with the point of maximum risk highlighted by the black aircraft icons. The middle plot is the altitude over time, with the dark aircraft showing the point of maximum risk, and the bottom plot shows the trajectory of horizontal separation distance on the x axis and the altitude separation in the y axis.*

mitigated in this paper by the position uncertainty models used, where the aircraft's position offset from the straight line propagated trajectory is allowed to vary according to a distribution. As such, the model assumptions cover the infinite variety of other paths that the aircraft could take from each time step (however, the probability density is primarily focused on deviations from a straight line path).

The model lends itself well to large-scale analysis of aircraft encounters within a region or country due to its fast computation speed. For example, surveillance data of all flights during each 24 h period can be gathered and pruned to identify encounters that meet some criteria of interest, e.g. those where the aircraft come closer than some threshold distance. These encounters can then be processed by the proposed model to estimate their collision risk and then further analysed to investigate risk trends both spatially (identifying areas where riskier encounters happen more frequently) and by underlying causes. Such analysis is useful for ANSPs and is planned to be conducted for the Australian domestic airspace to get detailed metrics for risk.

7. Conclusion

The proposed model offers an effective way to quantify the collision risk for any individual conflict. It accounts for the time to conflict including intervention, and the horizontal and vertical separations along the entire projected paths of the aircraft. The model considers practical limitations, offering adaptations

https://doi.org/10.1017/S0373463323000085 Published online by Cambridge University Press

that enable computationally efficient solutions to any encounter geometry. The model has many benefits: it is fast to compute resulting in scalability, the model has a strong mathematical foundation that actually estimates collision risk, and it follows well-established collision risk modelling principles meaning it is clearly applicable to ANSPs and other organisations in the aviation risk modelling industry.

Future developments are planned to apply the model to thousands of historic conflicts and use learning-based methods to classify types of conflict risk, and then find simpler statistical formulae for collision risk that remains coupled to the mathematical models. These statistical methods may vary depending on the conflict classification, but would provide very fast risk analysis for large data sets.

References

Aldis G. and Barry S. (2015). Fast evaluation of the Anderson-Hsu collision risk for a crossing track scenario. In: *SASP*, Vol. SASP-WGH-27-2015-Nov-Oklahoma-WP-03, ICAO.

Anderson D. (2000a). An extended methodology for ADS longitudinal separation standards. In: *ICAO, RGCSP 10/WP 7*, 1–16.

Anderson D. (2000b). A modified collision risk model for a crossing track separation methodology. In: *ICAO, RGCSP 10/WP 14*, 1–12.

Anderson D. (2003). A general distance-based collision risk model based on reliability theory. In: *SASP*, Vol. SASP-WGH-4-2003-Nov-Hawaii-WP-09, ICAO.

Anderson D. (2005). A collision risk model based on reliability theory that allows for unequal RNP navigational accuracy. In: *SASP*, Vol. SASP-WGH-7-2005-May-Montreal-WP-20, ICAO.

Anderson D. and Lin X. (1996). A collision risk model for a crossing track separation methodology. *Journal of Navigation*, **49**(3), 337–349.

Arnaldo R. M., Saez F., Garcia E. and Portillo Y. (2012). Probability of potential collision for aircraft encounters in high density airspaces. In: Magister, T. (ed.), *Advances in Air Navigation Services*. INTECH. Available at: http://cdn.intechopen.com/pdfs-wm/38072.pdf

Burki-Cohen J. (1995). *An analysis of tower (ground) controller-pilot voice communications*. Technical report DOT-VNTSC-FAA-95-41, Federal Aviation Administration.

Cardosi K. (1993a). *An analysis of en route controller-pilot voice communications*. Technical report DOT/FAA/RD-93/11, US Department of Transportation.

Cardosi K. M. (1993b). Time required for transmission of time-critical air traffic control messages in an en route environment. *The International Journal of Aviation Psychology*, **3**(4), 303–313. https://doi.org/10.1207/s15327108ijap0304_4

Cardosi K. M., Buerki-Cohen J., Boole P. W., Hourihan J. and Mengert P. (1995). *Analysis of pilot response time to time-critical air traffic control calls*. Technical report DOT-VNTSC-FAA-95-41, Federal Aviation Administration.

Cardosi K., Brett B. and Han S. (1997a). *Analysis of TRACON controller pilot voice communications*. Technical report DOT/FAA/AR-96/66, US Department of Transportation.

Cardosi K., Brett B. and Han S. (1997b). *An analysis of TRACON (terminal radar approach control) controller-pilot voice communications*. Technical report DOT/FAA/AR-96/66, US Department of Transportation.

Cardosi K., Brett B. and Han S. (1998). *Pilot-controller communication errors: An analysis of aviation safety reporting system (ASRS)*. Technical report DOT/FAA/AR-98/17, US Department of Transportation.

Chen H. (2010). *Required action time in aircraft conflict resolution*. Ph.D. thesis. Available at: https://hdl.handle.net/11299/92986

Eurocontrol (2015). *Risk analysis tool - RAT guidance material*. Technical report.

Gonda J., Saumsiegle W., Blackwell B. and Longo F. (2005). Miami controller-pilot data link communications summary and assessment. In: *3rd USA/Europe Air Traffic Management R&D Seminar*, Italy, Napoli (June 2000).

Hsu D. A. (1981). The evaluation of aircraft collision probabilities at intersecting air routes. *Journal of Navigation*, **34**(1), 78–102.

ICAO (2008). *Performance-based navigation manual*. Technical report Doc 9613.

ICAO (2013). *Global operational data link document (GOLD)*. Technical report, ICAO, Montreal, Canada.

ICAO (2017). *Manual on monitoring the application of performance-based horizontal separation minima*. Technical report Doc 10063.

ICAO (2019). *Operating procedures & practices for regional monitoring agencies in relation to the use of a 300 m (1000 ft) vertical separation minimum between FL 290 and FL 410 inclusive (Doc 9937)*. Technical report Doc 9937.

Kovacova M., Licu A. and Lintner T. (2018). Aerospace performance factor and its potential advances. *MATEC Web of Conferences*, **236**, 1007.

Kuchar J. K. and Yang L. C. (2000). A review of conflict detection and resolution modeling methods. *IEEE Transactions on Intelligent Transportation Systems*, **1**(4), 179–189.

Morrow D., Lee A. and Rodvold M. (1993). Analysis of problems in routine controller-pilot communication. *The International Journal of Aviation Psychology*, **3**(4), 285–302. https://doi.org/10.1207/s15327108ijap0304_3

Netjasov F. (2012). Framework for airspace planning and design based on conflict risk assessment: Part 2: Conflict risk assessment model for airspace tactical planning. *Transportation Research Part C: Emerging Technologies*, **24**, 213–226.

Nickelson M. (2018). *Aircraft response latencies to ATC clearances*. In: *SASP*, Vol. SASP-2-2018-May-Montreal-WP-28, ICAO. Note.

Parker J. I. (2019). *Airborne risk identification and assessment*. Technical report, MITRE.

Prinzo O. (1993). *ATC pilot voice communications—A survey of the literature*. Technical report DOT/FAA/AM-93/20, US Department of Transportation.

Prinzo O. and McClellan M. (2005). *Terminal radar approach control: Measures of voice communications system performance*. Technical report DOT/FAA/AM-05/19, US Department of Transportation.

Rantanen E. M., McCarley J. S. and Xu X. (2004). Time delays in air traffic control communication loop: Effect on controller performance and workload. *The International Journal of Aviation Psychology*, **14**(4), 369–394. https://doi.org/10.1207/s15327108ijap1404_3

Reich P. (1966a). Analysis of long-range air traffic systems: Separation standards ii. *Journal of Navigation*, **19**(1), 88–98.

Reich P. (1966b). Analysis of long-range air traffic systems: Separation standards III. *Journal of Navigation*, **19**(3), 331–347.

Cite this article: Kallinen V, Barry S, McFadyen A (2023). Collision risk quantification for pairs of recorded aircraft trajectories. *The Journal of Navigation* **76**: 2–3, 181–199. https://doi.org/10.1017/S0373463323000085